

## EFFECT OF DIPHENYLPHOSPHINE IN THE SYNTHESIS OF PbSe NANOPARTICLES

L. M. DE LEON COVIAN<sup>ab</sup>, J. A. ARIZPE ZAPATA<sup>ab</sup>,  
M. A. GARZA NAVARRO<sup>ab</sup>, D. I. GARCIA GUTIERREZ<sup>ab</sup>

<sup>a</sup>*Facultad de Ingeniería Mecánica y Eléctrica, FIME, Universidad Autónoma de Nuevo León, UANL, Av. Universidad S/N, San Nicolás de los Garza, N. L., C.P. 66450, México*

<sup>b</sup>*Centro de Innovación, Investigación y Desarrollo en Ingeniería y Tecnología, CIIDIT, Universidad Autónoma de Nuevo León, UANL, Parque PIIT Km. 10 de la Nueva Autopista al Aeropuerto Internacional de Monterrey, Apodaca, N. L., C.P. 66600, México*

PbSe nanoparticles (NPs) were synthesized varying the amount of diphenylphosphine (DPP) added (0, 0.05 and 0.1 ml) to the selenium precursor (TOP-Se to 97%), with a reaction time of 15 minutes. Subsequently, the obtained PbSe NPs were characterized using transmission electron microscopy (TEM) to assess the effect of the variation of the DPP on their morphology, size, crystal structure and yield of the reaction. Increasing the amount of DPP in the reaction produced smaller nanoparticles, with better size distribution and increased the yield of the reaction. The optical properties were evaluated using UV-Vis-NIR spectroscopy, in order to obtain the first absorption peak of the NPs, and from this value calculate the energy band gap ( $E_g$ ); which showed a correlation with the average size measured on each sample, as it has been reported on the literature. Additionally, this study settles the basis for a better understanding of the role of DPP in the synthesis of PbSe nanoparticles, and provides a guideline for proper selection of the ratio Pb/DPP used in the synthesis.

(Received September 25, 2014; Accepted November 5, 2014)

*Keywords:* PbSe nanoparticles, Diphenylphosphine

### 1. Introduction

Semiconductors in the form of nanoparticles (NPs) present several advantages over those in bulk form. One of these advantages being the dependency of the nanoparticles' optical and electronic properties on their size and morphology. Thus, these properties can be controlled by changing the size and morphology of the nanoparticles during their reaction synthesis. Semiconductor lead chalcogenide nanoparticles, such as PbSe, have been intensively investigated for their potential applications in the area of alternative energy sources, particularly solar energy [1-6], as light absorbing material for third generation solar cells. Parameters such as temperature, molar ratio of Pb/Se, concentration and type of capping agent, growth time and precursor types, are very important in the synthesis of PbSe nanoparticles. When any of these parameters is modified, nanostructured species of PbSe, with different sizes and morphologies, can be produced: 0D structures such as spherical NPs [7-9]; star shaped NPs [10, 11]; cubic NPs [8, 12, 13, 14]; and 1D structures such as nanowires [10, 12]. These parameters affect the absorption wavelength of the resultant nanostructures [9].

---

\* Corresponding author: [domingo.garciagt@uanl.edu.mx](mailto:domingo.garciagt@uanl.edu.mx)

Various references [15-18] indicate that the addition of diphenylphosphine (DPP) increases the production of PbSe NPs and, hence, the nucleation rate [17]. Another important issue that arises when using trioctylphosphine-selenium (TOP-Se) (97%), along with DPP, as precursors for the synthesis of PbSe nanostructures, is the improvement in the reproducibility of the reaction, compared to using only TOP-Se (90 %) without DPP [2,9,18]. This occurs due to the impurities of various secondary phosphines (i.e. dioctylphosphine and dibutylphosphine) in the TOP-Se (90%) [16].

Various mechanisms for PbSe synthesis have been proposed, such as that reported by Steckel et al. [17], where they state that there are two possible reaction mechanisms. One in which the TOP-Se (97%) reacts with  $\text{Pb}^{2+}$  to produce trioctylphosphine oxide (TOPO), an oleate anhydride and PbSe monomers; the center of lead remains as  $\text{Pb}^{2+}$ , while selenium is released as  $\text{Se}^{2-}$ . And the other one in which the  $\text{Pb}^{2+}$  is reduced by the DPP to form the  $\text{Pb}^0$  and diphenylphosphine oxide (DPPO), subsequently, the  $\text{Pb}^0$  reacts with TOP-Se to release the TOP and form the PbSe, however this second mechanism occurs at longer reaction times. Accordingly, Garcia-Gutierrez et al. [19] proposed a mechanism of nucleation and subsequent formation of PbSe NPs by reducing  $\text{Pb}^{2+}$  (from the lead oleate) to  $\text{Pb}^0$ , the reducing agents being the secondary phosphines, like DPP. This occurs at short reaction times, basically at the beginning of the reaction (1 to 8 min), and using a stoichiometric ratio of  $\text{Pb}/\text{Se}=1/1$  and using TOP-Se (90%). Another proposed mechanism is that stated by Evans et al. [16]. In their work, the authors report that the secondary phosphines, in particular the DPP, are responsible for the formation of PbSe NPs, mainly because when the pure TOP-Se (99.3%, distillate product) is added to the synthesis, the PbSe NPs are not formed, whereas when adding a specific amount of DPP, PbSe nanoparticles start to appear in the reaction, while the DPP start to disappear; until, eventually, it completely disappears. These authors did not report the formation of  $\text{Pb}^0$  in the aforementioned synthesis. Both Steckel et al. [17] and Evans et al. [16] based their work in NMR spectroscopy analysis, where this technique was used to elucidate the organic components present in the synthesis product, not directly the characteristics (size, morphology, size distribution) of the PbSe nanoparticles or the effect that varying the synthesis conditions had on these characteristics.

In this paper PbSe NPs were synthesized by varying the volume of DPP added (0, 0.05 and 0.1 ml) to the reaction, while keeping the other parameters constant, to assess its effect on the characteristics of the synthesized PbSe nanoparticles. Afterwards, a detailed analysis of morphology, size and crystalline structure was performed by transmission electron microscopy (TEM) to make a correlation with the variation of DPP concentration. The absorption wavelength, corresponding to the first exciton formation, was determined for the different experiments using UV-Vis-NIR spectroscopy. Additionally, a qualitative analysis for the yield of the reaction, related to the amount of PbSe nanoparticles produced was also performed. It is worth to mention that this study contributes on a better understanding of the synthesis mechanisms of PbSe nanoparticles and provide a guideline for proper selection of the ratio  $\text{Pb}/\text{DPP}$  used for its preparation.

## 2. Experimental Section

**Preparation of Se precursor.** Trioctylphosphine-Se (TOP-Se to 97%) 1M was prepared by adding 1.974 g of Se to a volumetric flask of 25 ml, heated on a plate with magnetic stirring for about 2 hours at 50°C (until the solution became completely clear). This solution was allowed to stir overnight. The preparation and storage of Se precursor were carried out under inert atmosphere ( $\text{N}_2$ ) in a glovebox. The working conditions for the preparation of TOP-Se were taken from reference [9]. The TOP was used as received. The purity of the TOP used in the experiments was 97%; since many reports in the literature use this level of purity, or even lower (90%).

**Lead precursor preparation (lead oleate) and PbSe nanoparticles.** For the synthesis of lead precursor (lead oleate), 0.446 g of  $\text{PbO}$ , 1.63 ml of oleic acid (OA) and 23.4 ml of 1-octadecene (ODE) were added into a three-necked flask. Resultant dissolution was heated to 170°C and kept at this temperature for 30 min, with a constant magnetic stirring. For the synthesis of the PbSe nanoparticles, the temperature of the reactor was lowered to 150°C. Once the temperature was stable (150°C), 4.05 ml of TOP-Se were rapidly added to the dissolution of lead

oleate, along with specific amounts of DPP (0, 0.05 or 0.1 ml, depending on the experiment). It is worth to mention that immediately after the TOP-Se was added to the reactor, the PbSe NPs began to form. After 15 minutes the reaction was stopped by adding 25 %v of chloroform and cooled in a cold water bath. PbSe NPs and lead oleate synthesis were performed under an atmosphere of  $N_2$ . The reaction was carried out using the following conditions: molar ratio of Pb/Se = 1/2; OA/Pb = 2.5/1; growth time of 15 min; and reaction temperature of 150°C. A post-treatment (cleaning) procedure was performed on the synthesized nanoparticles, in order to remove all the organic substances and unreacted products in the reaction. This procedure consisted of the precipitation of the NPs with methanol (30 ml) and acetone (10 ml); then, the NPs were redispersed in chloroform (approximately 1 ml). The procedure was repeated three times and then the nanoparticles were stored under inert atmosphere ( $N_2$ ) in a glovebox, for further characterization. Finally, once the TEM and optical characterizations were performed, the remaining dissolvent in the final product were slowly evaporated by heating the solution at 80°C during a week, in order to weigh the final product.

**Characterization.** The synthesized nanoparticles were characterized by transmission electron microscopy (TEM), in a FEI TEM Titan G<sup>2</sup> 80-300 microscope, operated at 300 kV, with Scanning-Transmission Electron Microscopy (STEM) capabilities and equipped with a High Angle Annular Dark Field (HAADF) detector from Fishione; a Bright Field (BF) and an Annular Dark Field (ADF) STEM detectors from Gatan; and EDAX energy dispersive X-ray spectrometer (EDXS). For the optical characterization, an Agilent UV-Vis-NIR Cary 5000 spectrometer, with a detection range from 175 nm to 3300 nm, was used.

### 3. Results and Discussion

**Shape and size evolution relative to the amount of DPP added.** Figure 1 shows BF images obtained from the sample that was synthesized without the addition of DPP. In Figures 1(a) and (b) it is possible to observe the formation of large NPs along with smaller ones. Larger NPs lack a defined morphology and display a size of approximately 10 nm [see Figure 1(a)], whereas the smaller ones have a size of approximately 3 nm [see Figure 1(b)]. As it has been reported previously, these large and small particles are known to be PbSe and metallic Pb NPs, respectively [19]. Furthermore, the size distribution of PbSe NPs is somewhat heterogeneous, although the size distribution of Pb NPs seems to be homogeneous. The size histogram for the PbSe nanoparticles in this reaction is shown in Figure 4(a), this reaction presented an average nanoparticles size of 10.28 nm with a standard deviation of 0.93 nm.

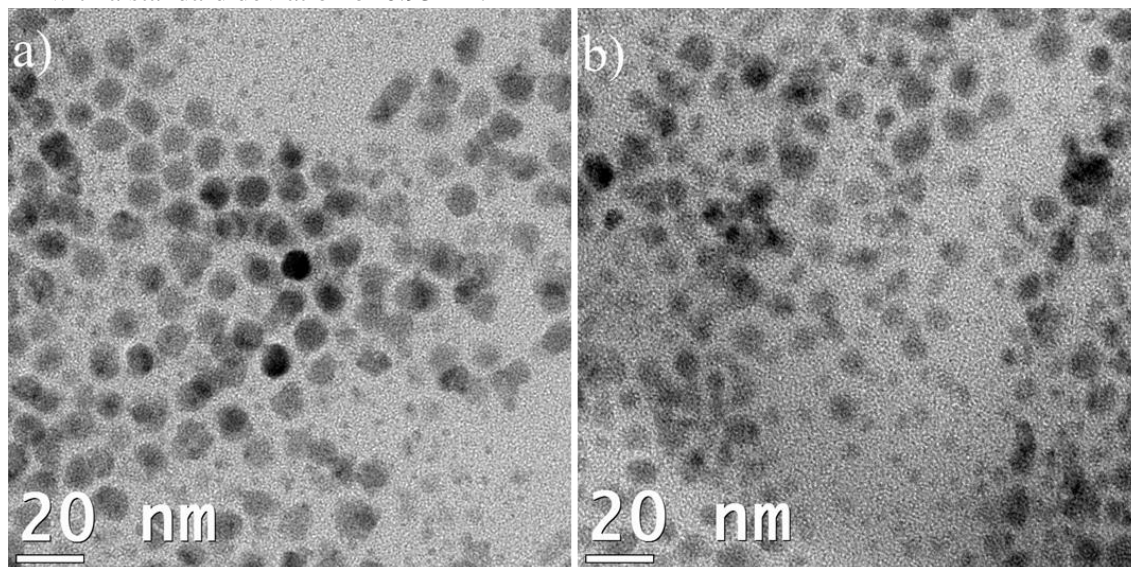


*Fig. 1. a) and b) BF-TEM images of the synthesized nanoparticles obtained with no DPP added to the reaction*

As Figure 2 displays, the addition of 0.05 ml of DPP to the reaction largely promotes the formation of PbSe NPs that have quasi-spherical [see Figure 2(a)] and polyhedral shapes [see Figure 2(b)], and an average size of 8.43 nm on the nanoparticles that didn't coalesce. Most of the analyzed areas showed a homogeneous particle distribution, although there were few zones in which PbSe NPs were observed to coalesce [see Figure 2(b)]. The size histogram for this reaction is shown in Figure 4(b), where an average nanoparticles size of 8.43 nm was obtained, with a standard deviation of 0.67 nm, on the nanoparticles that didn't coalesce.

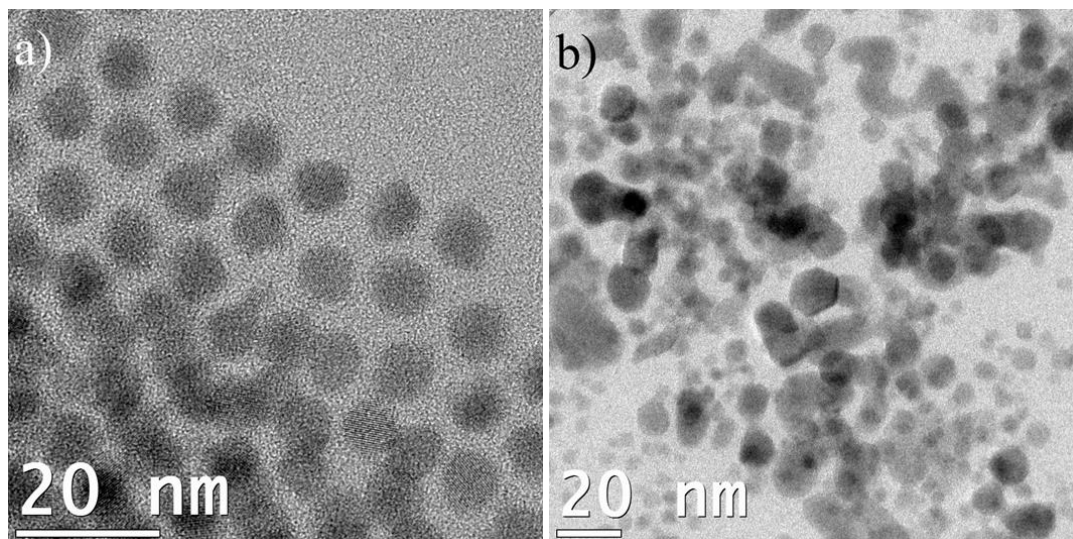


*Fig. 2. a) y b) BF-TEM images of the synthesized nanoparticles obtained with 0.05 ml of DPP added to the reaction*

A clear improvement in morphology and size distribution is obtained by adding 0.1 ml of DPP. The morphology is nearly spherical and polyhedral, with an average size of 8.72 nm; in this synthesis no presence of metallic Pb NPs was observed (see Figure 3). The size histogram for this reaction is shown in Figure 4(c), where an average size of 8.72 nm was obtained with a standard deviation of 0.54 nm. Based on these observations, for this series of experiments, the synthesis that displayed a higher control on nanoparticles' size and morphology was the one with the highest DPP concentration.

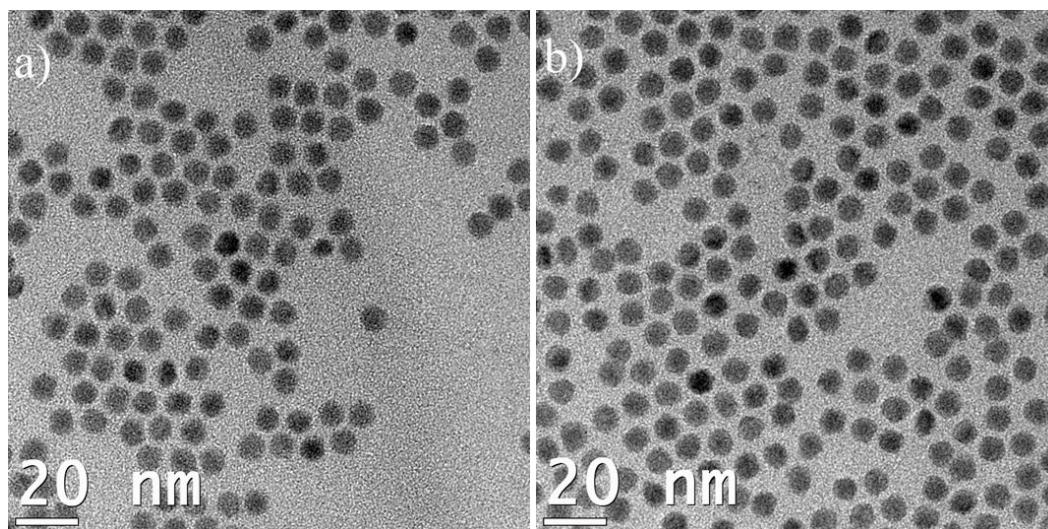


*Fig. 3. a) y b) BF-TEM images of the synthesized nanoparticles obtained with 0.1 ml of DPP added to the reaction*

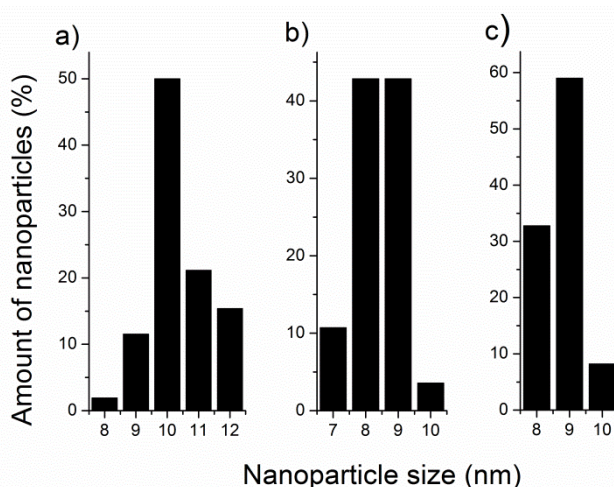


Fig. 4. Histogram of the PbSe nanoparticles from the experiment with a) no DPP, b) 0.05 ml DPP and c) 0.1 ml DPP added to the reaction

**Crystalline structure.** The crystal structure of PbSe NPs was obtained by SAED (Selected Area Electron Diffraction) and HR-TEM (High Resolution - TEM) studies. SAED patterns and HRTEM images were acquired for all three experiments, although in the present section just the results for the sample with 0.1 ml of DPP are shown (see Figure 5). Figure 5(a) depicts the indexed SAED pattern obtained from the PbSe nanoparticles. Herein is possible to identify reflections related to the families of planes  $\{111\}$ ,  $\{200\}$ ,  $\{220\}$ ,  $\{222\}$ ,  $\{420\}$  and  $\{422\}$  of the FCC crystalline structure reported for PbSe (see JCPDS card #: 06-0356 [21]). Figure 5(c) shows the HRTEM image of a PbSe nanoparticle, where lattice resolution can be clearly resolved. In this image, an interplanar distance of approximately 3.6 Å can be observed. This distance can be associated to the  $\{111\}$  family planes of this crystal structure. The same results were observed in the other two experiments, which confirm the crystal structure of the nanoparticles synthesized in all three experiments.

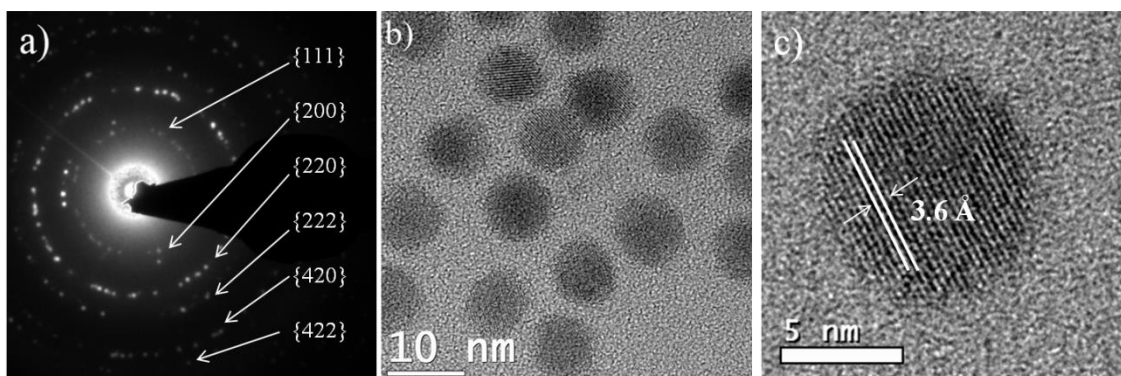


Fig. 5. a) SAED pattern of PbSe NPs, b) BF-TEM of several PbSe nanoparticles, and c) HRTEM image of one PbSe nanoparticle, in this image clear lattice resolution can be observed, and an interplanar spacing of 3.6 Å can be resolved

**Determination of the band gap energy,  $E_g$ .** As it has been widely reported [7,20], when changing the size of the NPs, they exhibit a variation in their optical properties, mainly due to quantum confinement effects. The most evident absorption peaks in the UV-Vis-NIR spectra of PbSe nanoparticles are due to the generation of the first Bohr exciton in these nanostructures. Figure 6 shows the UV-Vis NIR spectra for the samples with 0 ml, 0.05 ml and 0.1 ml of DPP.

The wavelengths of each experiment were consistent with those reported for PbSe nanoparticles, with average sizes corresponding to those observed in the different samples [9]. Also, the behavior related to the quantum confinement effect, where a decrement on the wavelength associated to the generation of the first Bohr exciton is related to the decrement in the nanoparticles average size. Additionally, the band gap energy of the PbSe nanoparticles was calculated from the UV-Vis-NIR absorbance spectra of the different samples, following the methodology reported in reference [22]. Table 1 shows the band gap energy calculated for the different samples.

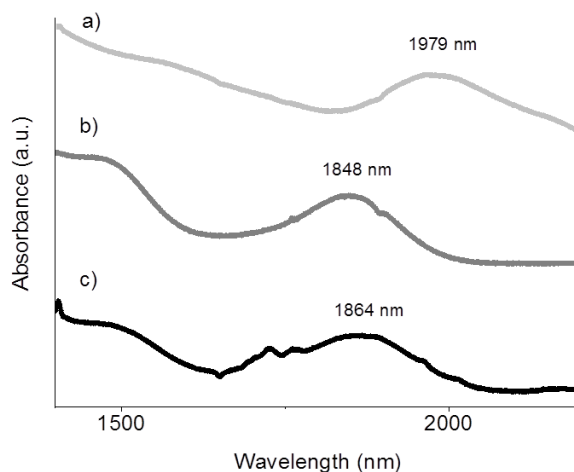


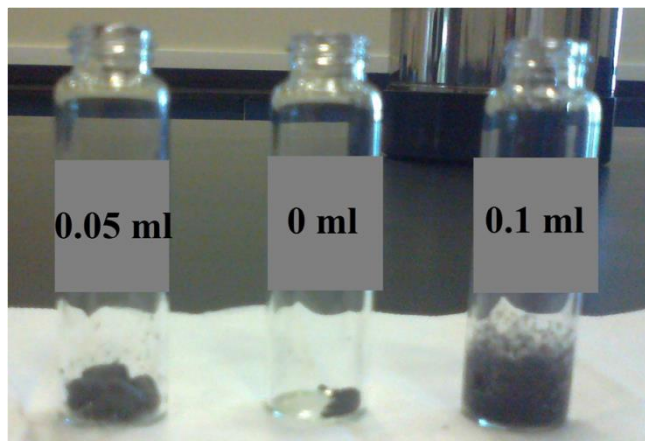
Fig. 6. UV-Vis-NIR spectra of PbSe nanoparticles with a) 0.0 ml, b) 0.05 ml and c) 0.1 ml of DPP

Table 1. Wavelengths and band gap energies ( $E_g$ ).  
\* Considering only nanoparticles that did not coalesce

DPP Volume (ml)	NPs size (nm)	Wavelength (nm)	Band gap (eV)
0	10.28	1979	0.52
0.05	8.43*	1848	0.63
0.1	8.72	1864	0.62

**Dependency of yield of the reaction on amount of DPP added.** From the presented experimental evidence, it is possible to state that the addition of DPP during the synthesis of PbSe nanoparticles increases the yield of the reaction; hence increasing the number of nanoparticles produced. In order to verify the increment on the quantity of synthesized PbSe NPs, we carried out both qualitatively (through simple observation) and quantitatively (by weighing the NPs) measurements.

Accordingly, Figure 7 shows a picture of three glass vials containing the synthesized NPs with 0.05 ml, 0.0 ml and 0.1 ml, respectively. A lower quantity of final product can be observed when no DPP is added during the synthesis of PbSe NPs, compared with those syntheses that were performed adding DPP (0.05 and 0.1 ml). This feature suggests the production of fewer nanoparticles when less DPP is used. In addition, when the amount of DPP added to the reaction increased, there was an increment in the yield of the reaction as well; since there was an increment of 11 % in the sample prepared with 0.1 ml of DPP with respect the samples prepared with 0.05 ml. It is worth to mention that the samples were weighted after they were purified and the remaining dissolvent was slowly evaporated during a week.



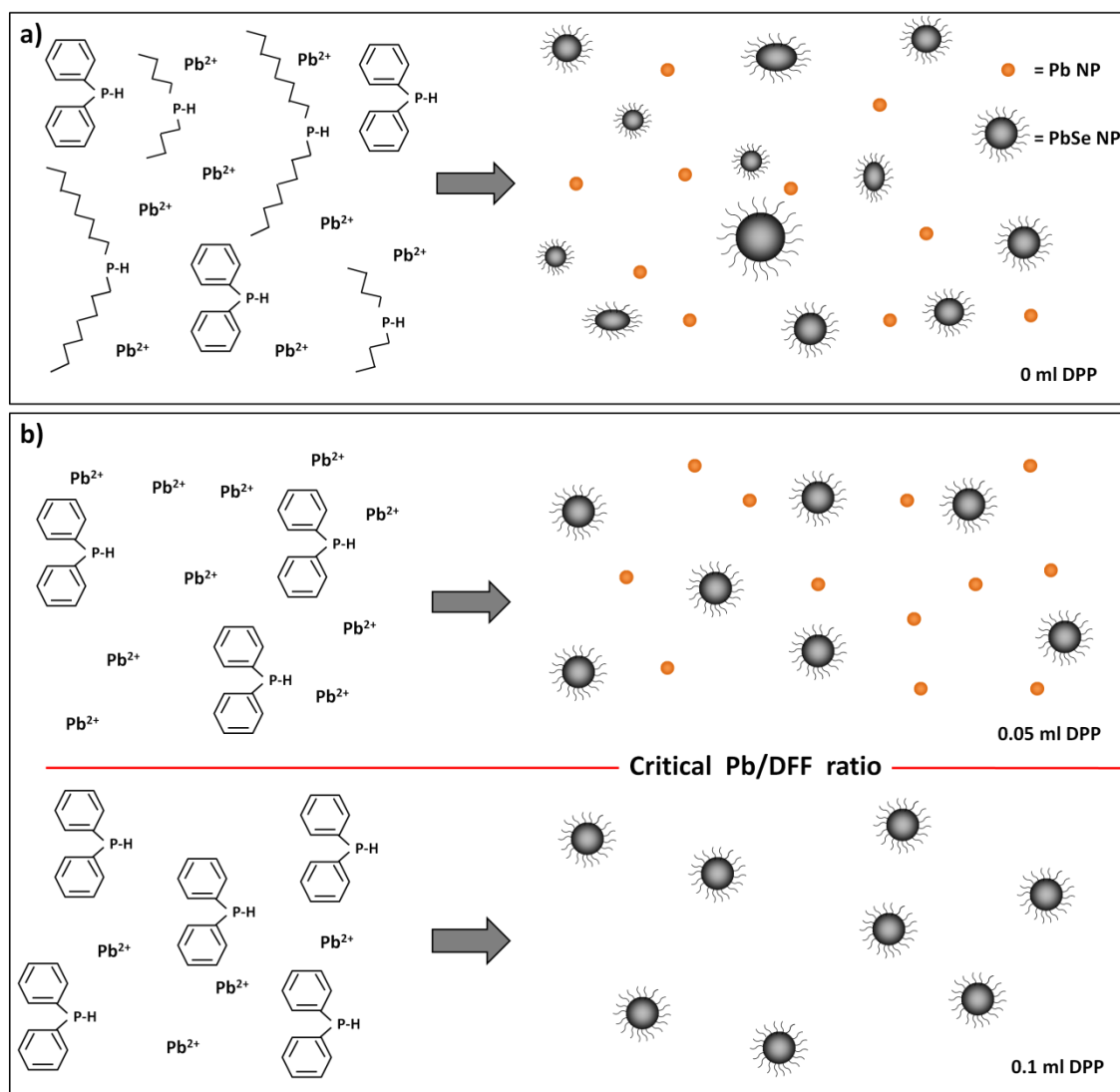
*Fig. 7. Image of the total amount of final product obtained in the three different syntheses of PbSe NPs with 0.05, 0.0 and 0.1 ml of DPP, respectively*

These variations on the quantity, morphology and crystallinity of the synthesized NPs could be explained as follows. First, the TOP (97%) used in this study did not go through any purification process before been used, in contrast to what has been reported by Evans [16]. In the latter work, the authors report, prior to the purification of the TOP (97%), the existence of various secondary phosphines (i.e. dioctylphosphine and dibutylphosphine, among others), which could be related to the heterogeneity in the size distribution of the experiment with no DPP added (see Figure 1b). This heterogeneity in size distribution could be the result of the presence of various secondary phosphines in the reaction. As the serial and parallel reactions that give way to the formation of monomers, and eventually nucleation centers of PbSe nanoparticles, take place; the presence of various types of secondary phosphines leads to multiple reaction rates, thus multiple nucleation rates. This produces PbSe NPs with different sizes at the final phase of the synthesis, as depicted in Scheme 1 a). However, when a significant amount of only one secondary phosphine (i.e. DPP) is added, the NPs obtained will have very similar sizes, namely a more homogeneous distribution.

Secondly, a relevant observation made on the experiments with no DPP and 0.05 ml of DPP, is the presence of metal  $Pb^0$  NPs at the end of the reaction (after 15 minutes of growth time). These Pb nanoparticles are considered to be impurities in the reaction, since it is desired that the entire Pb used as a precursor ends up forming, solely, the PbSe nanoparticles. However, these Pb NPs are not observed in the experiment with 0.1 ml of DPP. Based on the experimental results, a relationship is identified between the presence of the  $Pb^0$  NPs after long reaction times and the addition of DPP in the reaction. The amount of metallic  $Pb^0$  NPs, for long reaction times, decreases with increasing amount of DPP added, and for the conditions used in the present study (15 minutes of reaction time) they disappear with the addition of 0.1 ml. This suggests that there is an inverse relationship between the amount of DPP added and the amount of  $Pb^0$  NPs observed at the end of the reaction (lead not incorporated into the PbSe nanoparticles). This result settle the basis for a higher control on the synthesis of PbSe nanoparticles, it indicates that increasing the amount of DPP in the reaction leads to shorter reaction times with higher amount of Pb forming the lead chalcogenide nanoparticle, and higher reaction yields.

Finally, in the current experiments adding 0.1 ml of DPP ensured the entire usage of Pb in the formation of the PbSe nanoparticles. This observations suggest that there will be a relationship between the reaction time and a ratio between the Pb and the DPP in which one of these reactants will be the limiting reactant and the other will be the excess reactant (if only these two species are compared). While the Pb precursor remains as the limiting reactant (for the reaction time chosen) the DPP will be the excess reactant, and no Pb nanoparticles will be observed in the final product of the reaction, as it is graphically illustrated in Scheme b). Otherwise, if the DPP is the limiting reactant and the Pb precursor is the excess reactant (for the same chosen reaction time), Pb nanoparticles will be observed in the final reaction product (Scheme c). This particular

relationship between Pb and DPP, for a chosen reaction time, could be understood as a critical Pb/DPP ratio. Table 2 shows the molar ratio of Pb/DPP and indicates which specie is the limiting reactant in each case, for the parameters used in these experiments.



*Scheme 1. Scheme showing the relationship between the Pb and the DPP, and the critical Pb/DPP ratio, in the formation of Pb and PbSe nanoparticles*

*Table 2. Molar ratio Pb/DPP*

DPP volume(ml)	Molar ratio Pb/DPP	Limiting reactant
0.05	7	DPP
0.1	3.5	Pb

Accordingly, what can be observed in Figure 3 is that at the end of the synthesis the initial amount of Pb is consumed at the critical Pb/DPP ratio, producing PbSe nanocrystals and lead oleate, as the capping agent of these PbSe nanocrystals; and the remaining DPP in the reaction is consumed following the mechanism proposed by Evans et al. [16].

#### 4. Conclusions

PbSe nanoparticles were synthesized varying the amount of DPP added to the reaction. The nanoparticles that showed the best characteristics, regarding size, morphology and size and morphology distribution, were the ones synthesized with the highest amount of DPP used (0.1 ml). After 15 minutes of reaction, no metallic Pb nanoparticles were observed in the final product of this synthesis. The Pb nanoparticles that appear at lower DPP concentrations in the reaction can be understood as undesirable intermediate products of the synthesis. The addition of DPP in the reaction produces smaller PbSe nanoparticles, compared to same reaction times in synthesis where no DPP is added. This contributes to lowering the wavelength of their absorption peak, which is related to an increment in the energy of the nanoparticles' band gap. The calculated values for the  $E_g$  of the different synthesized nanoparticles match in good agreement with the values reported in the literature for PbSe nanoparticles of similar sizes. Not only the size of the nanoparticles gets reduced, but also its size distribution is improved, as it becomes more homogeneous. This same effect is observed in the shape of the nanoparticles, as the amount of DPP is increased its final shapes become more homogeneous. In addition, an increment in DPP also increased the yield of the reaction, producing higher amounts of PbSe nanoparticles with increased amount of DPP used. No clear effect of DPP was observed in the crystal structure of the nanoparticles. Finally, a relationship between the ratio between the Pb precursor and DPP was observed at a constant reaction time. There is a critical Pb/DPP ratio for the reaction that ensures the complete usage of the Pb in the formation of the PbSe nanoparticles, with Pb incorporated into the nanoparticles, either within the nanoparticles or in the capping layer. These results settle the basis for the optimization of synthesis methods that produce higher quantities of lead chalcogenide nanoparticles with improved characteristics, such as size and shape, as well as size and shape distributions.

#### Acknowledgements

This work was supported by the Mexican Secretary of Education (SEP), PROMEP program, through the project "Apoyo a la Incorporacion de Nuevos PTC", project number PROMEP/103.5/10/3889, and by CONACYT Mexico through projects number 148391 and 154303. LMDC and JAAZ thank and acknowledge the financial support received from CONACYT Mexico.

#### References

- [1] Y. Liu, M. Gibbs, J. Puthussery, S. Gaik, R. Ihly, H. W. Hillhouse, Law M. Nano Lett. **10**, 1960 (2010).
- [2] J. M. Luther, M. Law, Q. Song, C. L. Perkins, M. C. Beard, A. Nozik J. ACS Nano. **2**(2), 271 (2008).
- [3] JJ Choi, Y-F Lim, MB Santiago-Berrios, M Oh, B-R Hyun, L Sun, AC Bartnik, A Goedhart, GG Malliaras, HD Abruña, FW Wise, T. Hanrath Nano Lett. **9**(11), 3749 (2009).
- [4] D Cui, J Xu, T Zhu, G Paradee, S Ashok Appl Phys Lett. **88**, 183111 (2006).
- [5] WU Huynh, JJ Dittmer, AP. Alivisatos Science. **295**, 2425 (2002).
- [6] GI Koleilat, L Levina, H Shukla, SH Myrskog, S Hinds, AG Panttatyus-Abraham, EH. Sargent ACS Nano **2**(5), 833 (2008).
- [7] H. Du, Ch. Chen, R. Krishnan, T. D. Krauss, J. M. Harbold, F. W. Wise, M. G. Thomas, J. Silcox Nano Lett. **2**(11), 1321 (2002).
- [8] W. W. Yu, J. C. Falkner, B. S. Shih, V. L. Colvin Chem. Mater. **16**, 3318 (2004).
- [9] W. Lu, J. Fang, Y. Ding, Z. L. Wang J. Phys. Chem. B. **109**, 19219 (2005).
- [10] K. S. Cho, D. V. Talapin, W. Gaschler, Ch. Murray B. J. Am. Chem. Soc. **127**, 7140 (2005).
- [11] AJ Houtepen, R Koole, D Vanmaekelbergh, J Meeldijk, SGJ. Hickey J. Am. Chem. Soc.

- 128**, 6792 (2006).
- [12] E Lifshitz, M Bashouti, V Kloper, A Kigel, MS Eisen, S. Berger Nano Lett. **3**(6), 857 (2003).
- [13] M Achimovičová, N Daneu, A Rečnik, J Ďurišin, P Baláž, M Fabián, J Kováč, A Šatka. Chem Pap **63**(5): 562 (2009).
- [14] R Kerner, O Palchik, A Gedanken. Chem Mater **13**, 1413 (2001).
- [15] J. Joo, J. M. Pietryga, J. A. McGuire, S-H. Jeon, D. J. Williams, H-L. Wang, V. I. Klimov, A. J. Am. Chem. Soc. **131**, 10620 (2009).
- [16] Ch. M. Evans, M. E. Evans, T. D. Krauss J. Am. Chem. Soc. **132**, 10973 (2010).
- [17] J. S. Steckel, B. K. H. Yen, D. C. Oertel, M. G. Bawendi J. Am. Chem. Soc. **128**, 13032 (2006).
- [18] K. S. Leschkies, T. J. Beatty, M. S. Kang, D. J. Norris, E. S. Aydil ACS Nano. **3**(11), 3638 (2009).
- [19] D. I. Garcia-Gutierrez, L. M. De Leon-Covian, D. F. Garcia-Gutierrez, M. Treviño-Gonzalez, M. A. Garza-Navarro, S. Sepulveda-Guzman J Nanopart. Res. **15**, 1620 (2013).
- [20] J. E. Murphy, M. C. Beard, A. G. Norman, S. P. Ahrenkiel, J. C. Johnson, P. Yu, O. I. Mičić, R. J. Ellingson, A. J. Nozik J. Am. Chem. Soc. **128**, 3241 (2006).
- [21] Joint Committee on Powder Diffraction Standards, Number Card 06-0356.
- [22] D. A. Dholakia, G. K. Solanki, S. G. Patel, M. K. Agarwal Scientia Iranica, **10**(4), 373 (2003).